

fastMI: a fast and consistent copula-based estimator of mutual information

Soumik Purkayastha^a, Peter X.K. Song^{a,*}

^a*Department of Biostatistics, University of Michigan, Ann Arbor, MI 48109, USA.*

Abstract

As a fundamental concept in information theory, mutual information (MI) has been commonly applied to quantify association between random variables. Most existing estimators of MI have unstable statistical performance since they involve parameter tuning. We develop a consistent and powerful estimator, called fastMI, that does not incur any parameter tuning. Using a copula formulation, fastMI estimates MI by leveraging Fast Fourier transformation-based estimation of the underlying density. Extensive simulation studies reveal that fastMI outperforms state-of-the-art estimators with improved estimation accuracy and reduced run time for large data sets. fastMI not only provides a powerful test for independence that controls type I error, it may be used for further inference purposes. We establish asymptotic normality of fastMI for dependent random variables using a new data-splitting analytic argument. Anticipating that fastMI will be a powerful tool in estimating mutual information in a broad range of data, we develop an R package `fastMI` for broader dissemination.

Keywords: copula, kernel density estimation, Fast Fourier transformation, data-splitting inference, statistical dependence,

2020 MSC: Primary 62H12, Secondary 62F12

1. Introduction

Investigating dependence between two random variables is a key issue in statistical science. Classical measures like Pearson's r , Kendall's τ , and Spearman's ρ [8] serve as effective measures for linear or monotonic association, but are incapable of detecting non-linear association. More sophisticated measures, like the distance correlation (dCor) [30], the Heller-Heller-Gorfine (HHG) [10] statistic and the maximal information coefficient (MIC) [22] have been introduced to study more complex association patterns. These statistics demonstrate good theoretical properties as well as numerical performance. Recent studies have focused on mutual information (MI) [3], a remarkably general and intuitive measure of dependence. Originally introduced in a communication theory context [25], MI has seen widespread use in statistics, machine learning, with many exciting applications [33]. This widespread use is due in part to the self-equitability [13] of MI - the ability to characterize dependency strength for both linear and non-linear relationships between arbitrary random variables.

For continuous data, which shall be the focus of this paper, there are three distinct MI estimation approaches. The first approach implements a binning method to discretize continuous data into different bins and estimates MI from the discretized data [20, 29]. Success of this naive method depends heavily on proper specification of both number as well as position of said bins. Another approach is based on a k-nearest neighbors (kNN) estimation method, utilized by the Kraskov-Stögbauer-Grassberger (KSG) estimator [14]. As is the case with all kNN-based methods, the KSG estimator heavily depends on properly specifying the number of neighbors. The third approach is based on estimates of probability density functions, using histograms, kernel density estimation (KDE) [18], B-splines [6], or wavelets [21]. This approach relies on specifying a bandwidth parameter.

Although the approaches mentioned above demonstrate good numerical properties [6, 14, 18, 20, 21], the estimation processes are highly sensitive to proper specification of tuning parameter(s). As a consequence, the corresponding

*Corresponding author. Email address: pxsong@umich.edu

estimators may be unstable or exhibit serious bias issues. A recent study [36] presents a KDE-based approach in which the underlying bandwidth parameter H is first fixed, and a jackknifed version of MI (JMI) is proposed as a function of H . To free the estimation process from bandwidth selection, the authors propose maximising $JMI(H)$ over values of H , which serves as an estimator of MI. This method exhibits greater estimation efficiency than other MI estimation approaches, in addition to providing a stable test for independence that is more powerful than several popular methods like the dCor, HHG, or MIC. Based on existing literature, JMI serves as the current gold-standard for estimating MI, while providing a powerful and stable test of independence [36].

While JMI solves the problem of objectively choosing a bandwidth to obtain estimators of the true underlying density, it may not be optimal in the mean integrated squared error (MISE) sense, i.e., MISE of the estimated underlying density and the true density may not be minimized. An optimal solution for objectively choosing both the kernel shape and bandwidth that is computationally efficient and retains excellent statistical properties [1, 19] was presented recently. The resultant density estimator is optimal in the MISE sense. Using this density estimation approach, we propose a plug-in estimator of MI, the fastMI, that is established to be consistent and manyfold faster than JMI for large data sets. Instead of specifying a bandwidth parameter, the underlying estimation procedure chooses the bandwidth in a data-adaptive way that minimizes the MISE of the estimator and true underlying density. Further, we propose a test of independence based on fastMI.

Simulation studies comparing estimation accuracy reveal fastMI outperforms the gold standard JMI estimator. We compare the empirical power of fastMI with JMI when testing for independence and note superior performance of fastMI, especially for smaller sample sizes. We report a huge improvement in computation time of fastMI over JMI as well, in particular for larger data sets. Assuming dependence (i.e. when MI is not zero), we propose a novel data-splitting technique to establish root-n asymptotic normality of fastMI, allowing us to perform MI-based inference on large data sets. To the best of our knowledge, this key theoretical property does not extend to other estimators of MI. In summary, improved estimation efficiency, higher empirical power when testing for independence and reduced computation time demonstrate the superior performance of fastMI. Our findings establish that fastMI enjoys several appealing theoretical properties as well as stable numerical performance. While we present theory and applications for the bivariate case for ease of exposition, our method is equally applicable to multivariate structures.

2. Methods

2.1. Mutual information

Consider two random variables X and Y . Assuming existence of their joint probability density function (PDF) f_{XY} , MI is defined as

$$MI(X, Y) = \mathbb{E} \left\{ \frac{f_{XY}(X, Y)}{f_X(X)f_Y(Y)} \right\},$$

where f_X and f_Y are the marginal PDFs associated with X and Y respectively. MI is a true measure of association, i.e., it is equal to zero if and only if X and Y are independent and positive otherwise. Larger values of MI indicate stronger association. MI is invariant under monotonic transformations. Further, MI satisfies the self-equitability condition [36], indicating it detects associations without a bias for specific association patterns, unlike MIC [13]

2.2. Mutual information is copula entropy

From Sklar's theorem [5], we note that a bivariate PDF can be expressed in terms of an underlying copula density function and the product of the marginal densities as follows

$$c_{XY}(u_X, u_Y) = \frac{f_{XY} \{F_X^{-1}(u_X), F_Y^{-1}(u_Y)\}}{f_X \{F_X^{-1}(u_X)\} f_Y \{F_Y^{-1}(u_Y)\}}, \quad (1)$$

where F_X and F_Y are the cumulative distribution functions (CDFs) associated with X and Y . Using Equation 1, we note that MI is equal to the negative of the entropy of the copula density [16], given by

$$MI(X, Y) = -h(c) = \int_{[0,1]^2} c(u_X, u_Y) \log \{c(u_X, u_Y)\} du_X du_Y. \quad (2)$$

This frees the computation of MI from the marginal distributions and removes the need for faithfully capturing their properties in the estimation procedure. Copula-based estimators separate the relevant entropy from the irrelevant entropies, thereby reducing the estimation error. The separation of the copula from the marginals makes copula-based estimation methods robust to any marginal irregularity, in contrast with density dependent methods, such as the kNN-based KSG estimator. Recognizing MI as an integral in Equation 2, we may use classical Monte Carlo methods [23] for estimation purposes. However, we must first estimate the underlying copula density function c , which is discussed next.

2.3. Estimating non-parametric copulas

In order to estimate c , we must resolve the challenge in dealing with the closed support of a bivariate copula: the unit square $[0, 1]^2$. Typically, kernel estimators have problems with bounded support: for points close to the boundaries, they place some positive mass outside of the support. To address this problem, we apply a probit transformation to the copula density as follows

$$c_{XY}(u_X, u_Y) = \frac{f\{\Phi^{-1}(u_X), \Phi^{-1}(u_Y)\}}{\phi\{\Phi^{-1}(u_X)\}\phi\{\Phi^{-1}(u_Y)\}}, \quad (3)$$

where Φ is the standard normal CDF and ϕ its density. Thus, in order to estimate MI, we consider a kernel method for estimating f . In the probit-transformed domain, kernel estimators work well and do not suffer from boundary issues since the underlying density converges slowly to zero [24].

KDEs are commonly used techniques for estimating PDFs. The KDE method requires specification of some kind of bandwidth H or a kernel function K with a specific bandwidth. Selecting optimal H is a tricky issue and it calls for user-intervention for common use cases [26]. Further, tuning for H is computationally intensive, since it requires repeated density estimation. The difficulty compounds for higher dimensions [7]. A review of automatic selection methods [9] recommends a variety of different approaches that are dependent on data set characteristics (including sample size, smoothness, and skewness) and thus is hard to implement in practise. While the JMI provides an objective estimation method that does not require explicit specification of H , it yields estimates of MI that are maximised with respect to an underlying H . This approach does not guarantee accurate estimation of the underlying density, and may lead to larger MSEs in MI estimation. We shall discuss this drawback through simulation studies described in section 3.

An attractive alternative to the KDE-based estimation strategy involves Fourier transformation. We utilize a PDF estimation method that is computationally fast with excellent statistical properties. The density estimator so obtained, is called the self-consistent estimator (SCE), and is used to estimate MI. The SCE-based estimator of MI is called fastMI. The SCE-based approach presents a solution for objectively and optimally choosing both the kernel shape and bandwidth [1, 19] that is unencumbered by the need for user-selected parameters or tuning.

2.4. Self-consistent density estimation

Let us consider a random bivariate sample denoted by $\mathcal{S} = \{\mathbf{Z}_j = (X_j, Y_j) \in \mathcal{X} \times \mathcal{Y}, j = 1, 2, \dots, n\}$ from density f , which belongs to the Hilbert space of square integrable functions, given by

$$\mathcal{L}^2 = \left\{ f : \int f^2(\mathbf{z})d\mathbf{z} < \infty \right\}.$$

Without loss of generality, we assume $\mathcal{X} \times \mathcal{Y} = \mathbb{R}^2$. We consider the SCE $\hat{f} \in \mathcal{L}^2$. In order to define \hat{f} , we require a kernel function K , which belongs to the class of functions given by

$$\mathcal{K} := \left\{ K : K(\mathbf{z}) \geq 0 \forall \mathbf{z}; K(\mathbf{z}) = K(-\mathbf{z}) \forall \mathbf{z}; \int K(\mathbf{z})d\mathbf{z} = 1 \right\}.$$

Specifically, \hat{f} is given by the convolution of a kernel K and the set of delta functions centered on the dataset as follows:

$$\begin{aligned} \hat{f}(\mathbf{z}) &:= n^{-1} \sum_{j=1}^n K(\mathbf{z} - \mathbf{Z}_j), \mathbf{z} \in \mathbb{R}^2 \\ &= n^{-1} \sum_{j=1}^n \int_{\mathbb{R}^2} K(\mathbf{t})\delta(\mathbf{z} - \mathbf{Z}_j - \mathbf{t})d\mathbf{t}, \end{aligned} \quad (4)$$

where $\delta(\mathbf{z})$ is the Dirac delta function [15]. Our aim is identify the optimal kernel \hat{K} , where “optimal” is intended as minimising the mean integrated square error (MISE) between the true density f and the estimator \hat{f} :

$$\begin{aligned}\hat{K} &:= \operatorname{argmin}_{K \in \mathcal{K}} \operatorname{MISE}(\hat{f}, f) \\ &= \operatorname{argmin}_{K \in \mathcal{K}} \mathbb{E} \left[\int_{\mathbb{R}^2} \{\hat{f}(\mathbf{z}) - f(\mathbf{z})\}^2 d\mathbf{z} \right],\end{aligned}\tag{5}$$

where the \mathbb{E} operator denotes taking expectation over the entire support of f . The SCE in Equation 4 may be represented equivalently by its inverse Fourier transform pair, $\hat{\phi} \in \mathcal{L}^2$:

$$\hat{\phi}(\mathbf{t}) = \mathcal{F}^{-1}(\hat{f}(\mathbf{z})) = \kappa(\mathbf{t})C(\mathbf{t}),\tag{6}$$

where \mathcal{F}^{-1} represents the multidimensional inverse Fourier transformation from space of data $\mathbf{z} \in \mathbb{R}^2$ to frequency space coordinates $\mathbf{t} \in \mathbb{R}^2$. $\kappa = \mathcal{F}^{-1}(K)$ is the inverse Fourier transform of the kernel K and C is the empirical characteristic function (ECF) of the data, defined as

$$C(\mathbf{t}) = n^{-1} \sum_{j=1}^{n_1} \exp(it' \mathbf{Z}_j).\tag{7}$$

The optimal transform kernel $\hat{\kappa}$ that minimizes the MISE in Equation 11 is as follows [1, 19]

$$\hat{\kappa}(\mathbf{t}) = \frac{n}{2(n-1)} \left[1 + \sqrt{1 - \frac{4(n-1)}{|nC(\mathbf{t})|^2}} \right] I_{A_n}(\mathbf{t}).\tag{8}$$

Note that A_n serves as a low-pass Fourier filter that yields a stable estimator. We follow standard nomenclature [1] and denote A_n as the set of “acceptable frequencies”. For further discussion on A_n please see Section 1.3 of the Supplement.

The optimal transform kernel $\hat{\kappa}$ in Equation 8 may be anti-transformed back to the real space to obtain the optimal kernel \hat{K} , which also belongs to \mathcal{K} . The classical kernel estimation approach [26] assumes a specific form (such as the Gaussian kernel or Epanechnikov kernel) of the kernel K_H which depends on a bandwidth parameter H and requires tuning H according to some optimality criterion, like minimum MISE. In contrast, the SCE method does not make strong assumptions on the functional form of K . Rather, its estimate \hat{K} is determined entirely by a data-driven approach.

After stating the sufficient conditions for the estimator \hat{f} to converge to the true density f for $n \rightarrow \infty$, Theorem 4 establishes strong consistency of the estimator \hat{f} at all points on the support of f .

Theorem 1. *Let the true density f be square integrable and its corresponding Fourier transform ϕ be integrable, then the self consistent estimator \hat{f} , which is defined by Equation 4 - Equation 8 converges almost surely to f as $n \rightarrow \infty$, under the additional assumptions $\mathcal{V}(A_n) \rightarrow \infty$, $\mathcal{V}(A_n)/\sqrt{n} \rightarrow 0$ and $\mathcal{V}(\bar{A}_n) \rightarrow 0$ as $n \rightarrow \infty$. Further, assuming f to be continuous on support \mathbb{R}^2 , we have uniform almost sure convergence of \hat{f} to f as $n \rightarrow \infty$.*

Proof: Here A_n represents the frequency filter that ensures a stable solution of the SCE \hat{f} . \bar{A}_n is the complement of A_n and the volume of A_n is given by $\mathcal{V}(A_n)$. The proof of Theorem 4 is given in Section S.1.4 of the Supplement.

Having obtained a consistent estimator \hat{f} , we consider Equation 2 and Equation 3 to obtain our fastMI estimator, given by

$$\widehat{MI}_{fast} = n^{-1} \sum_{j=1}^n \log \left[\hat{c}_{XY} \left\{ \hat{F}_X(X_j), \hat{F}_Y(Y_j) \right\} \right],\tag{9}$$

where \hat{F}_X and \hat{F}_Y are the empirical CDFs of X and Y respectively. The estimator so obtained is consistent, as established by Theorem 5

Theorem 2. *Let the assumptions of Theorem 4 hold. Further, we assume the true underlying copula function c_{XY} is bounded away from zero and infinity on its support. Then, the estimator \widehat{MI}_{fast} given by Equation 9 converges in probability to the true MI as $n \rightarrow \infty$.*

Proof: The proof of [Theorem 5](#) is given in Section S.2.1 of the Supplement.

On the basis of [Theorem 5](#), we can propose a permutation-based test for independence, i.e., a test for $H_0 : MI = 0$ against the alternative $H_a : MI > 0$. Since the null hypothesis specifies a value at the boundary of the parameter space (MI is always non-negative), the null distribution of $\sqrt{n}\widehat{MI}_{fast}$ is not asymptotically normal. However, assuming dependence, i.e., for $MI \neq 0$, we establish asymptotic normality of fastMI using a novel data-splitting argument. Note that the data-splitting technique is solely for statistical inference and not required for estimation purposes.

We split the data of size n into two disjoint sets, \mathcal{D}_1 and \mathcal{D}_2 with sample sizes n_1 and n_2 respectively ($n_1 + n_2 = n$). Using data from $\mathcal{D}_1 = \{(X_j^{\mathcal{D}_1}, Y_j^{\mathcal{D}_1})\}_{j=1}^{n_1}$ we obtain estimates of the copula density function $\hat{c}_{\mathcal{D}_1}$. Under some mild assumptions (see [Theorem 4](#)), we have proved uniform almost sure convergence of these estimators to their population counterparts on their respective support sets as sample size $n_1 \rightarrow \infty$. Using data from $\mathcal{D}_2 = \{(X_j^{\mathcal{D}_2}, Y_j^{\mathcal{D}_2})\}_{j=1}^{n_2}$, we then evaluate the data-splitting based estimator \widehat{MI}_{fast}^{DS} as follows

$$\widehat{MI}_{fast}^{DS} = n_2^{-1} \sum_{j=1}^{n_2} \log \left[\hat{c}_{\mathcal{D}_1} \left\{ \hat{F}_X(X_j^{\mathcal{D}_2}), \hat{F}_Y(Y_j^{\mathcal{D}_2}) \right\} \right]. \quad (10)$$

[Theorem 3](#) establishes asymptotic normality of \widehat{MI}_{fast}^{DS} as $n_1 \wedge n_2 := \min(n_1, n_2) \rightarrow \infty$.

Theorem 3. *Let the assumptions of [Theorem 5](#) hold. Further, we assume the true $MI \neq 0$. Under these assumptions, we have*

$$\sqrt{n_2} \left\{ \widehat{MI}_{fast}^{DS} - MI \right\} \xrightarrow{\mathcal{D}} N \left(0, \sigma_{MI}^2 \right),$$

as $n_1 \wedge n_2 \rightarrow \infty$, with $\sigma_{MI}^2 = \mathbb{V} \{ \log c(\mathbf{z}) \}$ denoting the asymptotic variance of the estimator.

Proof: The proof of [Theorem 3](#) is given in Section S.2.2 of the Supplement. Note that the sample size-based scaling factor associated with \widehat{MI}_{fast}^{DS} is linked with the sample size n_2 of the second data split \mathcal{D}_2 , rather than the entire combined sample $n = n_1 + n_2$. This is a consequence of the data splitting method we propose. However, we require $n_1 \wedge n_2 \rightarrow \infty$ while analysing the asymptotic behaviour of \widehat{MI}_{fast}^{DS} . We recommend splitting the data to create two data sets of (approximately) similar size, i.e., $(n_1 = n_2) \approx n/2$.

2.5. Test for independence

The estimator \widehat{MI}_{fast} may be used to test for independence between X and Y . Rejection rules of the test based on asymptotic theory require data with large sample sizes, which may not be always available in practice. To ensure a stable and reliable performance, we implement a permutation-based test as it can give a precise finite-sample distribution of the test statistic for even small samples [[17](#)]. For a random sample of n observations, $S = \{(X_j, Y_j)\}_{j=1}^n$, let $\{\delta(1), \delta(2), \dots, \delta(n)\}$ be a random permutation of $\{1, 2, \dots, n\}$. Based on δ -permuted data set $S_\delta = \{(X_j, Y_{\delta(j)})\}_{j=1}^n$, we calculate the corresponding estimate \widehat{MI}_{fast} . On repeating the above procedure r times, $\mathcal{T}_{perm} = \left\{ \widehat{MI}_{fast}^{\delta_r} \right\}_{r=1}^R$, a collection of estimates is obtained, which may be used to approximate the null distribution of \widehat{MI}_{fast} , under the null hypothesis $H_0 : X$ and Y are independent. At significance level α , we reject the null hypothesis when \widehat{MI}_{fast} based on the original data is greater than the $(1 - \alpha)$ th empirical quantile of \mathcal{T}_{perm} . If the null hypothesis is rejected, we may use [Theorem 3](#) to provide $100(1 - \alpha)\%$ confidence intervals for MI.

3. Simulation studies

3.1. Estimation of MI

In this section, we compare the efficiency of the fastMI estimator with that of the existing gold-standard estimator of MI, the JMI. Previous simulation studies [[36](#)] show that the JMI has the smallest mean-squared error (MSE) for a wide class of multivariate association patterns across different sample sizes, thereby indicating its superior performance. Through extensive simulation studies, we compare the MSE performance of fastMI with JMI for a wide range

of bivariate association patterns, for different sample sizes. We generate a sample of n observations drawn from a bivariate PDF f_{XY} on \mathbb{R}^2 , specified by the underlying copula and marginal densities. Since marginal densities do not play a role in determining underlying mutual information, we fix them to be standard normal densities across all models.

We restrict ourselves to three separate classes of copula models [5, 11] - the symmetric Gaussian copula and two asymmetric Archimedean copula - the Clayton and Gumbel copula. While the Clayton copula exhibits greater dependence in the negative tail, the Gumbel copula exhibits greater dependence in the positive tail. Each of these copula classes may be specified by fixing the underlying value of Kendall’s τ , which in turn, may be used to compute the underlying true MI [2]. For each of the three copula classes considered, we fix $\tau \in \{0, 0.1, 0.2, \dots, 0.9\}$ and generate $n \in \{100, 250, 500\}$ bivariate samples. The simulated data are used to compute both JMI and fastMI. The MSEs of both estimators for different models and sample sizes are calculated based on $r = 1000$ replications. Our findings are presented in Figure 1. We note that fastMI has appreciably lower MSE for all models and sample sizes considered, indicating its superior performance over JMI.

3.2. Test for independence

We compare the permutation-based tests proposed for both fastMI and JMI. For the same bivariate patterns as described in subsection 3.1, with $\tau \in \{0, 0.05, \dots, 0.50\}$ ($\tau = 0$ indicates independence), we plot the empirical power curves for tests at significance level $\alpha = 0.05$ and present our results in Figure 2. We note that fastMI reports the higher empirical power even for moderate sample sizes. This is an appreciable improvement on current MI estimation methods, since estimation based on modest amounts of data may be challenging [27]. Upon increasing sample size, both methods report similar empirical power. Overall, fastMI seems to be a more stable and more powerful test of independence when compared to JMI.

Previous replicable studies [36] have compared the performance of the JMI-based test with dCor, HHG, MIC-based tests and noted JMI appears to be the most stable test of independence. Since it performs better than JMI in almost all the simulation designs considered in this paper, we believe fastMI to be a stable and efficient estimator of MI that can test for independence with high power while exhibiting type I error control.

3.3. Computation time

Since estimating MI is a computationally intensive statistical method, we compare run times of both fastMI and JMI for various sample sizes. We report the mean and standard deviation of run time in Table 1. Note that JMI has a lower runtime than fastMI for smaller sample sizes, however as sample size increases, we notice a reversal in trend, with fastMI run times many fold smaller than those of JMI. This improvement in run time establishes fastMI as an attractive method for studying association in larger data sets.

4. Real data analysis

In a landmark paper on gene expression studies [28], the authors studied the expressions of $p = 6223$ yeast genes with the goal of identifying genes whose transcript levels oscillate during the cell cycle. In lay terms, this means that the expressions were studied over $n = 23$ successive time points, and the goal was to identify the genes for which the transcript levels follow an oscillatory pattern. Through this analysis, we wish to highlight the utility of tests of independence in detecting patterns, since the number of genes is so large that visual investigations are not feasible. We use a curated version [22] of the data set (available through the R package `minerva`) to study the power of fastMI in discovering genes with oscillating transcript levels, and compare its performance with the competing JMI-based test. The curated version drops all genes with missing observations, and made several other modifications [22]. The revised data set has $p = 4381$ genes. The sole purpose of the analysis that follows is to compare the performance of fastMI with JMI in being able to detect oscillatory patterns. For each test, p-values were obtained and a set of significant genes were selected using the Bonferroni correction method.

There are 35 genes that are identified by fastMI but not JMI, which are displayed in Figure 3. These genes exhibit a sharp oscillatory behavior, either over the entire period of observation or even a narrower window of observation. However, they were not selected by the JMI-based test. Based on our simulation studies, this may be because of two reasons, namely (i) reduced estimation error of fastMI over JMI across a wide range of signal strengths or (ii) higher

power of fastMI compared to JMI in detecting association even for weak association for small sample sizes. Further, fastMI also selects genes that show other kinds of patterns (it selects a total of 87 genes), but those are selected by the JMI-based test as well and therefore do not appear in this set of 35 genes that are selected exclusively by fastMI.

5. Discussion

In this paper we present a fast and consistent MI estimator based on non-parametric copulas. Through extensive simulation studies we have demonstrated that the method has several desirable features of a high-performance MI estimator, outperforming the current gold-standard, the JMI. The method is non-parametric, which means that assumptions about relationships in the data are not imposed. Second, the method is not sensitive to marginal distributions; rather, by virtue of its focus on the copula, it only takes into account the joint association between variables without suffering from potential irregularities in the marginal distribution. We overcome issues that plague bandwidth-based MI estimators, such as bandwidth selection and slow computation times for large data sets. fastMI relies on a data-adaptive Fast Fourier transformation-based approach to estimating underlying copula structures. Its run time is many fold faster than the JMI for large data sets. The fastMI exhibits reduced estimation error and provides a more powerful test of independence than JMI. Finally, using a novel data-splitting approach we present asymptotic theory that allows us to provide confidence intervals associated with MI and perform statistical inference.

Due to its adaptability to complex associations and robustness to sample size, fastMI will be generally applicable in a wide range of fields and will advance and enhance the impact of information theory in many domains. Investigations of biological problems in which data collection is constrained by insurmountable practical reasons and is both limited by the difficulty of estimating information accurately from limited samples and by the presence of complex non-linearities [24] will be of particular interest.

To encourage broader dissemination of our fastMI-based toolkit for estimation and testing purposes, we have developed an R package `fastMI` that is publicly available. We attribute the good performance of fastMI to two factors: (i) the definition of MI itself and (ii) our estimation method that enjoys several computational and theoretical advantages mentioned above.

6. Technical details

6.1. The optimal data-driven kernel

In this section we derive the optimal kernel estimation method associated with the estimate given in (6) of the main article, where “optimal” is intended as minimising the mean integrated square error (*MISE*) between the true density f and its estimator \hat{f} , given by

$$MISE(\hat{f}, f) = \mathbb{E} \left[\int_{\mathbb{R}^2} \{\hat{f}(\mathbf{x}) - f(\mathbf{x})\}^2 d\mathbf{x} \right], \quad (11)$$

where the \mathbb{E} operator denotes taking expectation over the entire support of f . Here we consider density for a continuous random vector. We assume that both the true density f and the kernel density estimate \hat{f} belong to the Hilbert space of square integrable functions (denoted by $\mathcal{L}^2 = \{f : \int f^2(\mathbf{x})d\mathbf{x} < \infty\}$). Originally presented in [34], this section builds on the framework of self-consistent density estimation discussed in [1] and [19].

6.1.1. Preparation

Let us consider a random sample of n_1 observations denoted by $\mathcal{S} = \{\mathbf{Z}_j : (X_j, Y_j) \in \mathcal{Z} = \mathcal{X} \times \mathcal{Y} \subseteq \mathbb{R}^2, j = 1, 2, \dots, n_1\}$, from density f . Without loss of generality, let the sample space $\mathcal{Z} = \mathbb{R}^2$. We consider a generic bivariate kernel density estimator $\hat{f}(\mathbf{x})$ (to be evaluated at any $\mathbf{x} \in \mathcal{X}$) based on a kernel function $K(\mathbf{x})$ which is symmetric with respect to $\mathbf{x} = \mathbf{0}$ and satisfies $\int K(\mathbf{x})d\mathbf{x} = 1$. Specifically, $\hat{f}(\mathbf{x})$ is given by the convolution of kernel K and the set of delta functions centered on the dataset,

$$\hat{f}(\mathbf{x}) = \frac{1}{n_1} \sum_{j=1}^{n_1} K(\mathbf{z} - \mathbf{Z}_j) = \frac{1}{n_1} \sum_{j=1}^{n_1} \int_{\mathcal{Z}} K(\mathbf{s})\delta(\mathbf{z} - \mathbf{Z}_j - \mathbf{t})d\mathbf{t}, \quad (12)$$

where $\delta(\mathbf{x})$ is the Dirac delta function [15]. Here $\delta(\mathbf{x})$ has the value zero everywhere except at $\mathbf{x} = \mathbf{0}$, where it is a spike of indeterminate magnitude:

$$\delta(\mathbf{x}) = \begin{cases} \rightarrow \infty, & \text{if } \mathbf{x} = \mathbf{0}, \\ 0, & \text{if } \mathbf{x} \neq \mathbf{0}; \end{cases}$$

and it is constrained to have an integral equal to unity $\int_{\mathbb{R}^2} \delta(\mathbf{x}) d\mathbf{x} = 1$. Intuitively, $\delta(\mathbf{x})$ may be viewed as the limit of a multivariate normal distribution as all elements of the covariance matrix approach zero.

Note that in this paper, barring some mild restrictions, the shape of the kernel K is not prefixed, but rather will be determined by a data-driven approach. Further, note that the kernel estimate given by Equation 12 does not depend on any bandwidth matrix \mathbf{H} . This is contrary to the traditional kernel density estimator with a preset kernel function given by

$$\hat{f}_{\mathbf{H}}(\mathbf{z}) = \frac{1}{n_1} \sum_{j=1}^{n_1} K_{\mathbf{H}}(\mathbf{z} - \mathbf{Z}_j), \quad \mathbf{z} \in \mathcal{Z},$$

where \mathbf{H} is a 2×2 bandwidth (or smoothing) matrix which is symmetric and positive definite, the prefixed kernel function K is a symmetric multivariate density, and $K_{\mathbf{H}}(\mathbf{z}) = |\mathbf{H}|^{-1/2} K(\mathbf{H}^{-1/2}\mathbf{z})$ ($|\mathbf{H}|$ denotes the determinant of \mathbf{H}). Standard kernel density estimation techniques involve first choosing, in advance, a certain shape for the kernel K and then searching for an optimal bandwidth \mathbf{H} [26] by a tuning method such as cross validation. Popular choices for the function K include the Epanechnikov kernel K_E given by

$$K_E(\mathbf{x}) \propto (1 - \mathbf{x}'\mathbf{x})\mathbb{I}(\mathbf{x}'\mathbf{x} \leq 1), \quad \mathbf{x} \in \mathbb{R}^2,$$

where \mathbf{x}' is denotes the transpose of a vector \mathbf{x} and the indicator function $\mathbb{I}(\mathbf{x}'\mathbf{x} \leq 1)$ equals unity if $\mathbf{x}'\mathbf{x} \leq 1$ and zero otherwise. Another popular choice is the Gaussian kernel K_G given by

$$K_G(\mathbf{x}) \propto \exp\left(-\frac{\mathbf{x}'\mathbf{x}}{2}\right), \quad \mathbf{x} \in \mathbb{R}^2.$$

See more details in [32].

6.1.2. Derivation of the Fourier transform-based optimal kernel.

Diverging from the classical kernel estimation approach presented by [26], in this paper we focus on obtaining the optimal shape of the kernel K directly. Thus our aim is to obtain \hat{K} - the estimated optimal kernel which minimises the *MISE* of \hat{f} given by Equation 11. To do so, we invoke the Wiener filter-based procedure for signal deconvolution [35] via the following Fourier transform of the unknown density f , denoted by ϕ :

$$\phi(\mathbf{t}) = \mathbb{E}\{\exp(it'X)\} = \int_{\mathcal{X}} \exp(it'\mathbf{x})f(\mathbf{x})d\mathbf{x}, \quad \mathbf{t} \in \mathbb{R}^2.$$

We denote the Fourier transform of the estimate \hat{f} by $\hat{\phi}$ and the Fourier transform of the unknown kernel K by κ . Given the estimated optimal transform kernel $\hat{\kappa}$, we may apply the convolution theorem [12] to Equation 12 and obtain $\hat{\phi}(\mathbf{t}) = \hat{\kappa}(\mathbf{t})C(\mathbf{t})$, where C is the (known) empirical characteristic function (ECF) given by

$$C(\mathbf{t}) = \frac{1}{n_1} \sum_{j=1}^{n_1} \exp(it'X_j), \quad \mathbf{t} \in \mathbb{R}^2.$$

Note that the *MISE* in Equation 11 corresponds to the mean-squared distance between the true density f and an estimate \hat{f} , in terms of the Euclidean metric in the Hilbert space of square integrable functions \mathcal{L}^2 (provided $f, \hat{f}, \phi, \hat{\phi} \in \mathcal{L}^2$). Applying Parseval's theorem [12] to rewrite the *MISE* in the Fourier space, we get

$$MISE(\hat{f}, f) = \frac{1}{(2\pi)^2} \mathbb{E}\left(\int_{\mathbb{R}^2} |\hat{\phi}(\mathbf{t}) - \phi(\mathbf{t})|^2 d\mathbf{t}\right). \quad (13)$$

Since the data are independent and identically distributed, according to [31], we have the first two moments of $C(\mathbf{t})$:

$$\mathbb{E}\{C(\mathbf{t})\} = \phi(\mathbf{t}), \quad \mathbb{V}(|C(\mathbf{t})|) = (1 - |\phi(\mathbf{t})|^2)/n_1, \quad \mathbf{t} \in \mathbb{R}^2.$$

Together, they yield $\mathbb{E}(|C(\mathbf{t})|^2) = |\phi(\mathbf{t})|^2 + (1 - |\phi(\mathbf{t})|^2)/n_1$. The \mathbb{E} and \mathbb{V} operator denote taking expectation and variance over the entire support of f . Note for any complex number $z = a + ib$, the Euclidean norm is given by $|z| = \sqrt{a^2 + b^2}$. We assume validity of interchanging the integral and expectation operators, and rewrite Equation 13 as follows:

$$MISE(\hat{f}, f) = \frac{1}{(2\pi)^2} \int_{\mathbb{R}^2} \left\{ (n_1)^{-1} |\kappa(\mathbf{t})|^2 (1 - |\phi(\mathbf{t})|^2) + |\phi(\mathbf{t})|^2 |1 - \kappa(\mathbf{t})|^2 \right\} d\mathbf{t}. \quad (14)$$

Since f is a PDF, we have $|\phi(\mathbf{t})| \leq 1 \forall \mathbf{t} \in \mathbb{R}^2$, implying non-negativity of the first term in Equation 14, which corresponds to the finite sample size error. Note that the second term does not depend on sample size n_1 . According to nomenclature introduced by [26], these two sources of error are known as the error variance (inversely proportional to n_1) and squared error bias, respectively. Since Equation 14 is quadratic in κ , we may obtain its global minimum by equating the functional derivative of $MISE$ with respect to κ to zero, and then solving for the optimal Fourier-transformed kernel κ_{OPT} , which takes the form

$$\kappa_{OPT}(\mathbf{t}) = \frac{n_1}{n_1 - 1 + |\phi(\mathbf{t})|^2}, \quad \mathbf{t} \in \mathbb{R}^2. \quad (15)$$

Using the expression for the transformed optimal kernel in Equation 15 and the convolution theorem [12], we obtain the optimal $\hat{\phi}$ given by

$$\hat{\phi}(\mathbf{t}) = \hat{\kappa}(\mathbf{t})C(\mathbf{t}) = \frac{n_1 C(\mathbf{t})}{n_1 - 1 + |\phi(\mathbf{t})|^2}, \quad \mathbf{t} \in \mathbb{R}^2, \quad (16)$$

where $\hat{\phi}$ may be recognised as the Fourier transform of the optimal density estimate \hat{f} . Equation 16 implies that for each $\mathbf{t} \in \mathbb{R}^2$,

$$\hat{\phi}(\mathbf{t}) \xrightarrow{a.s.} \phi(\mathbf{t}),$$

because $C(\mathbf{t}) \rightarrow \phi(\mathbf{t})$ and $|\phi(\mathbf{t})| \leq 1$. Intuitively this implies that while an infinite sample would reproduce the true density itself, for finite n_1 , the optimal estimate $\hat{\phi}$ downweights the frequencies that contribute less to the estimator of the true density - this procedure may be compared to smoothing.

6.1.3. Iterative procedure to obtain $\hat{\phi}$.

We implement an iterative procedure based on Equation 16 to obtain $\hat{\phi}(\mathbf{t})$ for a given sample of size n_1 , which requires a starting value $\hat{\phi}_0(\mathbf{t})$. The updating rule at the r -th step is given as follows:

$$\hat{\phi}_{r+1}(\mathbf{t}) = \frac{n_1 C(\mathbf{t})}{n_1 - 1 + |\hat{\phi}_r(\mathbf{t})|^2}, \quad r = 0, 1, \dots \quad (17)$$

$\hat{\phi}$ is obtained as the fixed point of the iteration described in Equation 17, and at convergence, the resulting estimator is denoted by $\hat{\phi}$. Having obtained $\hat{\phi}$, we can use the Fourier anti-transformation of the following form:

$$\hat{f}(x) = \frac{1}{(2\pi)^2} \int_{\mathbb{R}^2} \exp(-it'x) \hat{\phi}(\mathbf{t}) d\mathbf{t} \quad (18)$$

to obtain the optimal density estimate \hat{f} . Also, upon convergence of the iterative procedure, the solution $\hat{\phi}$ satisfies the quadratic equation $(n_1 - 1)|\hat{\phi}(\mathbf{t})|^2 + 1 = n_1|\hat{\phi}(\mathbf{t})|C(\mathbf{t})$. Solving for $\hat{\phi}$, we follow [1] to choose the following non-null solution:

$$\hat{\phi}(\mathbf{t}) = \frac{n_1 C(\mathbf{t})}{2(n_1 - 1)} \left[1 + \sqrt{1 - \frac{4(n_1 - 1)}{|n_1 C(\mathbf{t})|^2}} \right] \mathbb{I}_{A_{n_1}}(\mathbf{t}), \quad (19)$$

which is regarded as the stable solution, where A_{n_1} serves as a low-pass filter that ensures stability of the estimation process.

Remark 1. The purpose of the filter $\mathbb{I}_{A_{n_1}}(\mathbf{t})$ is to define a Fourier-based low-pass filter on the ECF $C(\mathbf{t})$ that yields a stable optimal estimate in the minimum MISE sense. Primarily, the set A_{n_1} is specified such that:

$$A_{n_1} = \left\{ \mathbf{t} \in \mathbb{R}^2 : |C(\mathbf{t})|^2 \geq C_{\min}^2 = \frac{4(n_1 - 1)}{n_1^2} \right\}. \quad (20)$$

Here, the primary filter is necessary in Equation 19 for stability of the estimation method because the lower bound C_{\min} can ensure a well-defined square root term in Equation 19 for $\hat{\phi}$. Moreover, according to [1], the set A_{n_1} may exclude an additional small subset of frequencies to produce a smoother density estimate \hat{f} . In order for \hat{f} to converge to the true density f as n_1 increases, we require that this set of additionally excluded frequencies must shrink, so that the set A_{n_1} of included frequencies grows with increasing n_1 .

Remark 2. According to [19], the multidimensional ECF $C(\mathbf{t})$ consists of a finite set of contiguous hypervolumes denoted by $\{HV_l^{n_1}\}_{l=1}^{k_{n_1}}$, where k_{n_1} is a finite integer. Each hypervolume permits “above-threshold” frequency values \mathbf{t} for which the constraint in Equation 20 holds. Note that at least one such contiguous hypervolume containing $\mathbf{t} = \mathbf{0}$ is guaranteed to exist since $C(\mathbf{0}) = 1$ due to normalisation and the primary filter A_{n_1} has a lower bound $C_{\min} \leq 1$. Following the suggestion by [19] we employ the lowest contiguous hypervolume filter, choosing the only hypervolume centered at $\mathbf{t} = \mathbf{0}$, which we denote as $HV_1^{n_1}$ for notational convenience. We make the following observations about $HV_1^{n_1}$:

1. The set of frequencies included in the lowest contiguous hypervolume filter are bounded above since they will always be contained within a finite-sized hypervolume around the origin.
2. The volume of the lowest contiguous hypervolume filter grows as the number of data points n_1 increases, implying more frequencies are included for larger sample sizes.

The resulting filter satisfies the convergence conditions described by [1]. Hence, we set $A_{n_1} = HV_1^{n_1}$, and study convergence of \hat{f} to the true f as n_1 increases. For notational convenience, let \bar{A}_{n_1} denote the complement set of A_{n_1} and $\mathcal{V}(A_{n_1})$ denote the volume of A_{n_1} .

6.1.4. Large sample behaviour of the optimal density estimator.

In this section we prove Theorem 4 which establishes strong consistency of the estimator \hat{f} to the true density f as $n_1 \rightarrow \infty$ at all points on the support of f .

Theorem 4. Let the true density f be square integrable and its corresponding Fourier transform ϕ be integrable. Under the assumptions $\mathcal{V}(A_{n_1}) \rightarrow \infty$, $\mathcal{V}(A_{n_1})/\sqrt{n_1} \rightarrow 0$ and $\mathcal{V}(\bar{A}_{n_1}) \rightarrow 0$ as $n \rightarrow \infty$, we have the estimate \hat{f} , as defined by Equation 18, converging almost surely to the true density f as $n_1 \rightarrow \infty$.

Note the frequency filter A_{n_1} , its complement \bar{A}_{n_1} and its volume $\mathcal{V}(A_{n_1})$ are described in Remarks 1 and 2. Since the true density f and the estimator \hat{f} are both square-integrable, we can express them in terms of their corresponding Fourier transforms ϕ and $\hat{\phi}$ respectively. Since the characteristic function is integrable, we have, $\int |\phi(\mathbf{t})| d\mathbf{t} < \infty$. Through the following sequence of inequalities, we are able to establish an upper bound for the absolute error $|\hat{f}(\mathbf{x}) - f(\mathbf{x})|$ for any $\mathbf{x} \in \mathcal{X}$. By definition, note that $\hat{\phi}(\mathbf{t}) = 0$ for $\mathbf{t} \notin A_{n_1}$. To establish Theorem 4, it is sufficient to show that the upper bound of the absolute error given below tends to zero as $n_1 \rightarrow \infty$. We have:

$$\begin{aligned} |\hat{f}(\mathbf{x}) - f(\mathbf{x})| &= \left| \frac{1}{(2\pi)^2} \int_{\mathbb{R}^2} \exp(-i\mathbf{t}'\mathbf{x}) \{\hat{\phi}(\mathbf{t}) - \phi(\mathbf{t})\} d\mathbf{t} \right| \\ &\leq \frac{1}{(2\pi)^2} \int_{\mathbb{R}^2} |\exp(-i\mathbf{t}'\mathbf{x})| |\hat{\phi}(\mathbf{t}) - \phi(\mathbf{t})| d\mathbf{t} = \frac{1}{(2\pi)^2} \int_{\mathbb{R}^2} |\hat{\phi}(\mathbf{t}) - \phi(\mathbf{t})| d\mathbf{t} \\ &= \frac{1}{(2\pi)^2} \int_{A_{n_1}} |\hat{\phi}(\mathbf{t}) - \phi(\mathbf{t})| d\mathbf{t} + \frac{1}{(2\pi)^2} \int_{\bar{A}_{n_1}} |\phi(\mathbf{t})| d\mathbf{t} \\ &\leq \frac{1}{(2\pi)^2} \int_{A_{n_1}} |\hat{\phi}(\mathbf{t}) - C(\mathbf{t})| d\mathbf{t} + \frac{1}{(2\pi)^2} \int_{A_{n_1}} |C(\mathbf{t}) - \phi(\mathbf{t})| d\mathbf{t} + \frac{1}{(2\pi)^2} \int_{\bar{A}_{n_1}} |\phi(\mathbf{t})| d\mathbf{t} \\ &:= D_1 + D_2 + D_3. \end{aligned} \quad (21)$$

Under the assumptions, $\lim_{n_1 \rightarrow \infty} \mathcal{V}(A_{n_1}) = \infty$ and $\lim_{n_1 \rightarrow \infty} \mathcal{V}(\bar{A}_{n_1}) = 0$. Consequently, the second term in Equation 21, $D_2 \rightarrow 0$ as $n_1 \rightarrow \infty$ due to Theorem 1 of [4]. Further, $D_3 \leq \mathcal{V}(\bar{A}_{n_1})/(2\pi)^2$, since $|\phi(t)| \leq 1$. Consequently, $D_3 \rightarrow 0$ as $n_1 \rightarrow \infty$.

To prove $D_1 \rightarrow 0$ as $n_1 \rightarrow \infty$, we first consider the two following disjoint sets,

$$\begin{aligned} B_{n_1}^+ &= \{t : |C(t)|^2 \geq 4(n_1 - 1)/n_1^2\}, \\ B_{n_1}^- &= \{t : |C(t)|^2 < 4(n_1 - 1)/n_1^2\}. \end{aligned}$$

Using Equation 19, we rewrite the first integral D_1 as follows

$$\begin{aligned} D_1 &= \frac{1}{2\pi} \int_{A_{n_1} \cap B_{n_1}^+} |C(t)| \left(1 - \frac{n_1}{2(n_1 - 1)} \left[1 + \sqrt{1 - \frac{4(n_1 - 1)}{|n_1 C(t)|^2}} \right] dt \right) + \frac{1}{2\pi} \int_{A_{n_1} \cap B_{n_1}^-} |C(t)| dt \\ &:= D_4 + D_5. \end{aligned}$$

The first term D_4 may be simplified by noting that for $t \in B_{n_1}^+$, we have $|C(t)|^2 \geq 4(n_1 - 1)/n_1^2$. This ensures a non-negative argument under the square root operation. Using the inequality $\sqrt{1-x} + \sqrt{x} \geq 1$ for $0 \leq x \leq 1$ for D_4 , and using the inequality

$$|C(t)| \leq \sqrt{4(n_1 - 1)/n_1^2} \text{ for } t \in B_{n_1}^-,$$

we establish that D_1 is bounded as follows:

$$\begin{aligned} D_1 &= D_4 + D_5 \\ &\leq \frac{1}{(2\pi)^2} \int_{A_{n_1} \cap B_{n_1}^+} \left\{ \frac{1}{\sqrt{n_1 - 1}} - \frac{|C(t)|}{n_1 - 1} \right\} dt + \frac{\sqrt{4(n_1 - 1)}}{n_1(2\pi)^2} \int_{A_{n_1} \cap B_{n_1}^-} dt \\ &\leq \frac{1}{(2\pi)^2} \left\{ \frac{1}{\sqrt{n_1 - 1}} + \frac{1}{n_1 - 1} \right\} \int_{A_{n_1} \cap B_{n_1}^+} dt + \frac{\sqrt{4(n_1 - 1)}}{n_1(2\pi)^2} \int_{A_{n_1}} dt \\ &= \frac{1}{(2\pi)^2} \left\{ \frac{1}{\sqrt{n_1 - 1}} + \frac{1}{n_1 - 1} \right\} \mathcal{V}(A_{n_1} \cap B_{n_1}^+) + \frac{\sqrt{4(n_1 - 1)}}{n_1(2\pi)^2} \mathcal{V}(A_{n_1} \cap B_{n_1}^-) \\ &\leq \frac{1}{(2\pi)^2} \left\{ \frac{1}{\sqrt{n_1 - 1}} + \frac{1}{n_1 - 1} + \frac{\sqrt{4(n_1 - 1)}}{n_1} \right\} \mathcal{V}(A_{n_1}) \\ &\leq \frac{1}{(2\pi)^2} \left\{ \frac{1}{\sqrt{n_1 - 1}} + \frac{1}{n_1 - 1} + \frac{2}{\sqrt{n_1 - 1}} \right\} \mathcal{V}(A_{n_1}). \end{aligned} \tag{22}$$

The assumptions in Theorem 4 include $\mathcal{V}(A_{n_1})/\sqrt{n_1} \rightarrow 0$ as $n_1 \rightarrow \infty$, which ensures that the upper bound in Equation 22 tends to zero for large n_1 . In summary, assuming $\mathcal{V}(A_{n_1}) \rightarrow \infty$, $\mathcal{V}(\bar{A}_{n_1}) \rightarrow 0$, and $\mathcal{V}(A_{n_1})/\sqrt{n_1} \rightarrow 0$ as $n_1 \rightarrow \infty$, we have $|\hat{f}(x) - f(x)| \rightarrow 0$ for every $x \in \mathcal{X}$.

6.2. Large sample properties of \widehat{MI}_{fast} and \widehat{MI}_{fast}^{DS}

In this section we prove consistency of \widehat{MI}_{fast} as well as asymptotic normality of data-splitting based \widehat{MI}_{fast}^{DS} .

6.2.1. Consistency of \widehat{MI}_{fast}

Theorem 5. *Let the assumptions of Theorem 4 hold. Further, we assume the true underlying copula function c_{XY} is continuous and bounded away from zero and infinity on its support. Then, the estimator \widehat{MI}_{fast} converges in probability to the true MI as $n \rightarrow \infty$.*

From Theorem 4 we know that for any small ϵ , there exists a large enough N such that $\sup_z |\hat{c}(z) - c(z)| < \epsilon$. Using Taylor series expansion to $\log \{\hat{c}(z_i)/c(z_i)\}$, we get $\log \{\hat{c}(z_i)\} = \log \{c(z_i)\} + \frac{\hat{c}(z_i) - c(z_i)}{c(z_i)} + o(\epsilon)$, where we ignore the last

term. Summing the expression above over n observations, we get

$$\begin{aligned} \left| \widehat{MI}_{fast} - MI_{oracle} \right| &= \left| \frac{1}{N} \sum_{i=1}^N \log \{ \hat{c}(\mathbf{z}_i) \} - \frac{1}{N} \sum_{i=1}^N \log \{ c(\mathbf{z}_i) \} \right| \\ &\leq \frac{1}{N} \sum_{i=1}^n \left| \frac{\hat{c}(\mathbf{z}_i) - c(\mathbf{z}_i)}{c(\mathbf{z}_i)} \right| \leq \frac{\sup_i |\hat{c}(\mathbf{z}_i) - c(\mathbf{z}_i)|}{C} < \frac{\epsilon}{C}. \end{aligned}$$

Hence, as MI_{oracle} is consistent for MI, we can claim \widehat{MI}_{fast} is consistent for MI as well.

6.2.2. Asymptotic normality of $\sqrt{n_2} \widehat{MI}_{fast}^{DS}$

In this section we analyze the large-sample behaviour of \widehat{MI}_{fast}^{DS} using a data-splitting technique. This technique splits the available data \mathcal{D} , of size n , into two disjoint sets, resulting in \mathcal{D}_1 and \mathcal{D}_2 with sample sizes n_1 and n_2 respectively ($n_1 + n_2 = n$). We require that both $n_1, n_2 \rightarrow \infty$ as $n \rightarrow \infty$, or $n_1 \wedge n_2 := \min(n_1, n_2) \rightarrow \infty$. As described in ??, data from \mathcal{D}_1 is used to obtain estimates of the copula density function $\hat{c}_{\mathcal{D}_1}$ and the marginal density functions $\hat{f}_{X:\mathcal{D}_1}$ and $\hat{f}_{Y:\mathcal{D}_1}$. Under some mild assumptions, these density estimators converge uniformly to their population counterparts on their respective support sets as sample size $n_1 \rightarrow \infty$. See [Theorem 4](#) for more details. Using data from \mathcal{D}_2 we evaluate the estimator \widehat{MI}_{fast}^{DS} . Likewise, we define the oracle estimators based on the true density function as follows:

$$MI_{oracle} = (n_2)^{-1} \sum_{j=1}^{n_2} \log \{ c(\mathbf{Z}_j^{D_2}) \}. \quad (23)$$

The following theorem establishes a key result involving our plug-in estimators and oracle estimators in [Equation 23](#) under the data splitting technique.

Theorem 6. *Suppose the conditions presented in [Theorem 4](#) hold and that the true copula density c is smooth and bounded away from zero and infinity on their respective support. Thus, as $n_1 \wedge n_2 \rightarrow \infty$, we have:*

$$\sqrt{n_2} \left(\widehat{MI}_{fast}^{DS} - MI_{oracle} \right) \xrightarrow{\mathcal{P}} 0. \quad (24)$$

First, note that

$$\sqrt{n_2} \left(\widehat{MI}_{fast}^{DS} - MI_{oracle} \right) = \frac{1}{\sqrt{n_2}} \sum_{j=1}^{n_2} \frac{\hat{c}_{\mathcal{D}_1}(\mathbf{Z}_j^{D_2}) - c(\mathbf{Z}_j^{D_2})}{c(\mathbf{Z}_j^{D_2})} + o_{\mathcal{P}}(1) = \frac{S_{n_2}}{\sqrt{n_2}} + o_{\mathcal{P}}(1).$$

We now show that the leading term $S_{n_2}/\sqrt{n_2} \xrightarrow{\mathcal{P}} 0$ as $n_1 \wedge n_2 \rightarrow \infty$, which will establish the theorem. It is sufficient to show $\mathbb{E} \left\{ \left(S_{n_2}/\sqrt{n_2} \right)^2 \right\} \rightarrow 0$ as $n_1, n_2 \rightarrow \infty$. Note that $\mathbb{E} \left\{ \left(S_{n_2}/\sqrt{n_2} \right)^2 \right\} = \mathbb{E}^2 \left(S_{n_2}/\sqrt{n_2} \right) + \mathbb{V} \left(S_{n_2}/\sqrt{n_2} \right)$. First, we prove $\mathbb{E} \left(S_{n_2}/\sqrt{n_2} \right) = 0$. This is because

$$\begin{aligned} \mathbb{E} \left(\frac{S_{n_2}}{\sqrt{n_2}} \right) &= \mathbb{E}_{\mathcal{D}_1} \left\{ \mathbb{E}_{\mathbf{Z}|\mathcal{D}_1} \left(\frac{S_{n_2}}{\sqrt{n_2}} \middle| \mathcal{D}_1 \right) \right\} \\ &= \mathbb{E}_{\mathcal{D}_1} \left\{ \mathbb{E}_{\mathbf{Z}|\mathcal{D}_1} \left(\frac{1}{\sqrt{n_2}} \sum_{j=1}^{n_2} \frac{\hat{c}_{\mathcal{D}_1}(\mathbf{Z}_j^{D_2}) - c(\mathbf{Z}_j^{D_2})}{c(\mathbf{Z}_j^{D_2})} \middle| \mathcal{D}_1 \right) \right\} \\ &= \mathbb{E}_{\mathcal{D}_1} \left\{ \sqrt{n_2} \mathbb{E}_{\mathbf{Z}|\mathcal{D}_1} \left(\frac{\hat{c}_{\mathcal{D}_1}(\mathbf{Z}) - c(\mathbf{Z})}{c(\mathbf{Z})} \middle| \mathcal{D}_1 \right) \right\}, \end{aligned}$$

where the inner expectation term is evaluated as follows

$$\mathbb{E}_{\mathbf{Z}|\mathcal{D}_1} \left(\frac{\hat{c}_{\mathcal{D}_1}(\mathbf{Z}) - c(\mathbf{Z})}{c(\mathbf{Z})} \middle| \mathcal{D}_1 \right) = \int_{\mathbf{z}} \left(\frac{\hat{c}_{\mathcal{D}_1}(\mathbf{z}) - c(\mathbf{z})}{c(\mathbf{z})} \right) c(\mathbf{z}) d\mathbf{z} = \int_{\mathbf{z}} \hat{c}_{\mathcal{D}_1}(\mathbf{z}) d\mathbf{z} - \int_{\mathbf{z}} c(\mathbf{z}) d\mathbf{z} = 0.$$

The last equality holds since $\hat{\phi}_{\mathcal{D}_1}$ is the Fourier transform associated with the optimal density function estimator $\hat{c}_{\mathcal{D}_1}$, and an examination of [Equation 19](#) yields $\hat{\phi}_{\mathcal{D}_1}(\mathbf{0}) = 1$ and consequently, $\mathbb{E}(S_{n_2}/\sqrt{n_2}) = 0$. Next, we consider the term $\mathbb{V}(S_{n_2}/\sqrt{n_2})$, which may be expressed as follows:

$$\mathbb{V}\left(\frac{S_{n_2}}{\sqrt{n_2}}\right) = \mathbb{E}_{\mathcal{D}_1} \left\{ \mathbb{V}_{\mathbf{Z}|\mathcal{D}_1} \left(\frac{S_{n_2}}{\sqrt{n_2}} \middle| \mathcal{D}_1 \right) \right\} + \mathbb{V}_{\mathcal{D}_1} \left\{ \mathbb{E}_{\mathbf{Z}|\mathcal{D}_1} \left(\frac{S_{n_2}}{\sqrt{n_2}} \middle| \mathcal{D}_1 \right) \right\}, \quad (25)$$

where the second term is already shown to be zero. Note that, conditional on \mathcal{D}_1 , the terms $\hat{c}(\mathbf{Z}_j^{D_2})$ are independent and identically distributed for all $\mathbf{Z}_j^{D_2} \in \mathcal{D}_2$.

We have

$$\begin{aligned} \mathbb{V}_{\mathbf{Z}|\mathcal{D}_1} \left(\frac{S_{n_2}}{\sqrt{n_2}} \middle| \mathcal{D}_1 \right) &= \mathbb{V}_{\mathbf{Z}|\mathcal{D}_1} \left(\frac{1}{\sqrt{n_2}} \sum_{j=1}^{n_2} \frac{\hat{c}_{\mathcal{D}_1}(\mathbf{Z}_j^{D_2}) - c(\mathbf{Z}_j^{D_2})}{c(\mathbf{Z}_j^{D_2})} \middle| \mathcal{D}_1 \right) \\ &= \mathbb{V}_{\mathbf{Z}|\mathcal{D}_1} \left(\frac{\hat{c}_{\mathcal{D}_1}(\mathbf{Z}) - c(\mathbf{Z})}{c(\mathbf{Z})} \middle| \mathcal{D}_1 \right) = \mathbb{E}_{\mathbf{Z}|\mathcal{D}_1} \left\{ \left(\frac{\hat{c}_{\mathcal{D}_1}(\mathbf{Z}) - c(\mathbf{Z})}{c(\mathbf{Z})} \right)^2 \middle| \mathcal{D}_1 \right\}, \end{aligned}$$

since $\mathbb{E}_{\mathbf{Z}|\mathcal{D}_1} \left(\frac{\hat{c}_{\mathcal{D}_1}(\mathbf{Z}) - c(\mathbf{Z})}{c(\mathbf{Z})} \middle| \mathcal{D}_1 \right) = 0$. Moreover,

$$\mathbb{E}_{\mathbf{Z}|\mathcal{D}_1} \left\{ \left(\frac{\hat{c}_{\mathcal{D}_1}(\mathbf{Z}) - c(\mathbf{Z})}{c(\mathbf{Z})} \right)^2 \middle| \mathcal{D}_1 \right\} = \int_{\mathcal{Z}} \left(\frac{\hat{c}_{\mathcal{D}_1}(\mathbf{z}) - c(\mathbf{z})}{c(\mathbf{z})} \right)^2 c(\mathbf{z}) d\mathbf{z} \leq B \int_{\mathcal{Z}} (\hat{c}_{\mathcal{D}_1}(\mathbf{z}) - c(\mathbf{z}))^2 d\mathbf{z}.$$

where B is a (positive) lower bound for the density c over its support. Plugging this inequality into [Equation 25](#), we get

$$\mathbb{V}\left(\frac{S_{n_2}}{\sqrt{n_2}}\right) \leq B \times \mathbb{E}_{\mathcal{D}_1} \left\{ \int_{\mathcal{Z}} (\hat{c}_{\mathcal{D}_1}(\mathbf{z}) - c(\mathbf{z}))^2 d\mathbf{z} \right\} = B \times \text{MISE}(\hat{c}, c).$$

[1] present an expression of *MISE* in terms of the optimal kernel (as described in ??) and prove that the last expression goes to zero as sample size increases, i.e., $\text{MISE}(\hat{c}, c) \rightarrow 0$ as $n_1 \wedge n_2 \rightarrow \infty$. This allows us to claim $\sqrt{n_2} \left(\widehat{MI}_{fast}^{DS} - MI_{oracle} \right) \xrightarrow{\mathcal{P}} 0$ as $n_1 \wedge n_2 \rightarrow \infty$. Note that the arguments presented above are generally valid for any true density function that is bounded away from zero and infinity on its support. Using [Theorem 6](#) in conjunction with the following lemma, we arrive at asymptotic multivariate normality of \widehat{MI}_{fast}^{DS} .

Lemma 1. *By the central limit theorem we have, for $MI \neq 0$, the oracle estimator converging in distribution to a normal distribution, namely*

$$\sqrt{n_2} (MI_{oracle} - MI) \xrightarrow{\mathcal{D}} N(0, \sigma_{MI}^2), \text{ as } n_1 \wedge n_2 \rightarrow \infty, \quad (26)$$

where $\sigma_{MI}^2 = \mathbb{V}[\log\{c(\mathbf{Z})\}]$. This variance term may be estimated using standard Monte-Carlo methods.

Acknowledgments

We thank the Editor, Associate Editor and referees, as well as our financial sponsors.

References

- [1] A. Bernacchia, S. Pigolotti, Self-consistent method for density estimation, *Journal of the Royal Statistical Society: Series B (Statistical Methodology)* 73 (2011) 407–422.
- [2] M. Bolbolian Ghalibaf, Relationship between kendall’s tau correlation and mutual information, *Revista Colombiana de Estadística* 43 (2020) 3–20.
- [3] T. M. Cover, J. A. Thomas, *Elements of Information Theory*, Wiley, 2005.
- [4] S. Csörgő, V. Totik, On how long interval is the empirical characteristic function uniformly consistent?, *Acta Sci. Math. (Szeged)* 45 (1983) 141–149.
- [5] C. Czado, *Analyzing Dependent Data with Vine Copulas: A Practical Guide With R (Lecture Notes in Statistics, 222)*, Springer, paperback edition, 2019.
- [6] C. O. Daub, R. Steuer, J. Selbig, S. Kloska, *BMC Bioinformatics* 5 (2004) 118.
- [7] T. Duong, M. L. Hazelton, Cross-validation bandwidth matrices for multivariate kernel density estimation, *Scandinavian Journal of Statistics* 32 (2005) 485–506.
- [8] B. S. Everitt, A. Skronal, *The Cambridge dictionary of statistics*, Cambridge University Press, Cambridge, England, 4 edition, 2010.
- [9] N.-B. Heidenreich, A. Schindler, S. Sperlich, Bandwidth selection for kernel density estimation: a review of fully automatic selectors, *AStA Advances in Statistical Analysis* 97 (2013) 403–433.
- [10] R. Heller, Y. Heller, M. Gorfine, A consistent multivariate test of association based on ranks of distances, *Biometrika* 100 (2012) 503–510.
- [11] H. Joe, *Dependence Modeling with Copulas (Chapman & Hall/CRC Monographs on Statistics and Applied Probability)*, Chapman and Hall/CRC, hardcover edition, 2014.
- [12] D. W. Kammler, *A First Course in Fourier Analysis*, Cambridge University Press, 2008.
- [13] J. B. Kinney, G. S. Atwal, Equitability, mutual information, and the maximal information coefficient, *Proceedings of the National Academy of Sciences* 111 (2014) 3354–3359.
- [14] A. Kraskov, H. Stögbauer, P. Grassberger, Estimating mutual information, *Physical Review E* 69 (2004).
- [15] E. Kreyszig, *Advanced Engineering Mathematics*, Wiley, loose leaf edition, 2020.
- [16] J. Ma, Z. Sun, Mutual information is copula entropy, *Tsinghua Science and Technology* 16 (2008) 51–54.
- [17] B. F. Manly, *Randomization, Bootstrap and Monte Carlo Methods in Biology*, Chapman and Hall/CRC, 2018.
- [18] Y.-I. Moon, B. Rajagopalan, U. Lall, Estimation of mutual information using kernel density estimators, *Phys. Rev. E* 52 (1995) 2318–2321.
- [19] T. A. O’Brien, K. Kashinath, N. R. Cavanaugh, W. D. Collins, J. P. O’Brien, A fast and objective multidimensional kernel density estimation method: fastKDE, *Computational Statistics & Data Analysis* 101 (2016) 148–160.
- [20] L. Paninski, Estimation of entropy and mutual information, *Neural Computation* 15 (2003) 1191–1253.
- [21] A. M. Peter, A. Rangarajan, Maximum likelihood wavelet density estimation with applications to image and shape matching, *IEEE Transactions on Image Processing* 17 (2008) 458–468.
- [22] D. N. Reshef, Y. A. Reshef, H. K. Finucane, S. R. Grossman, G. McVean, P. J. Turnbaugh, E. S. Lander, M. Mitzenmacher, P. C. Sabeti, Detecting novel associations in large data sets, *Science* 334 (2011) 1518–1524.
- [23] C. P. Robert, *Monte Carlo Statistical Methods (Springer Texts in Statistics)*, Springer, paperback edition, 2010.
- [24] H. Safaai, A. Onken, C. D. Harvey, S. Panzeri, Information estimation using nonparametric copulas, *Physical Review E* 98 (2018).
- [25] C. E. Shannon, A mathematical theory of communication, *Bell System Technical Journal* 27 (1948) 379–423.
- [26] B. W. Silverman, *Density Estimation for Statistics and Data Analysis*, Chapman I& Hall, London, 1986.
- [27] T. Speed, A correlation for the 21st century, *Science* 334 (2011) 1502–1503.
- [28] P. T. Spellman, G. Sherlock, M. Q. Zhang, V. R. Iyer, K. Anders, M. B. Eisen, P. O. Brown, D. Botstein, B. Futcher, Comprehensive identification of cell cycle-regulated genes of the yeast *saccharomyces cerevisiae* by microarray hybridization, *Molecular Biology of the Cell* 9 (1998) 3273–3297.
- [29] S. P. Strong, R. Koberle, R. R. de Ruyter van Steveninck, W. Bialek, Entropy and information in neural spike trains, *Phys. Rev. Lett.* 80 (1998) 197–200.
- [30] G. J. Székely, M. L. Rizzo, N. K. Bakirov, Measuring and testing dependence by correlation of distances, *The Annals of Statistics* 35 (2007).
- [31] N. G. Ushakov, *Selected Topics in Characteristic Functions*, DE GRUYTER, 1999.
- [32] M. Wand, M. Jones, *Kernel Smoothing (Chapman & Hall/CRC Monographs on Statistics and Applied Probability)*, Chapman and Hall/CRC, hardcover edition, 1995.
- [33] Q. Wang, S. R. Kulkarni, S. Verdu, Divergence estimation for multidimensional densities via k -nearest-neighbor distances, *IEEE Transactions on Information Theory* 55 (2009) 2392–2405.
- [34] G. S. Watson, M. R. Leadbetter, On the estimation of the probability density, *The Annals of Mathematical Statistics* 34 (1963) 480–491.
- [35] N. Wiener, *Extrapolation, Interpolation, and Smoothing of Stationary Time Series*, The MIT Press, 1964.
- [36] X. Zeng, Y. Xia, H. Tong, Jackknife approach to the estimation of mutual information, *Proceedings of the National Academy of Sciences* 115 (2018) 9956–9961.

	$n = 250$	$n = 500$	$n = 1000$	$n = 2500$	$n = 5000$
JMI	0.112(0.02)	0.688(0.045)	2.969(0.179)	18.073(1.663)	71.938(4.076)
fastMI	0.313(0.115)	0.760(0.284)	2.481(1.141)	9.389(1.814)	20.387(0.269)

Table 1: Mean (standard deviation) run time of JMI and fastMI (in seconds).

Comparison of mean squared error (MSE) of competing mutual information (MI) estimation methods for various copula families.

The estimation methods compared here are Fast Fourier Transform–based MI (fastMI) and the jackknifed MI (JMI).

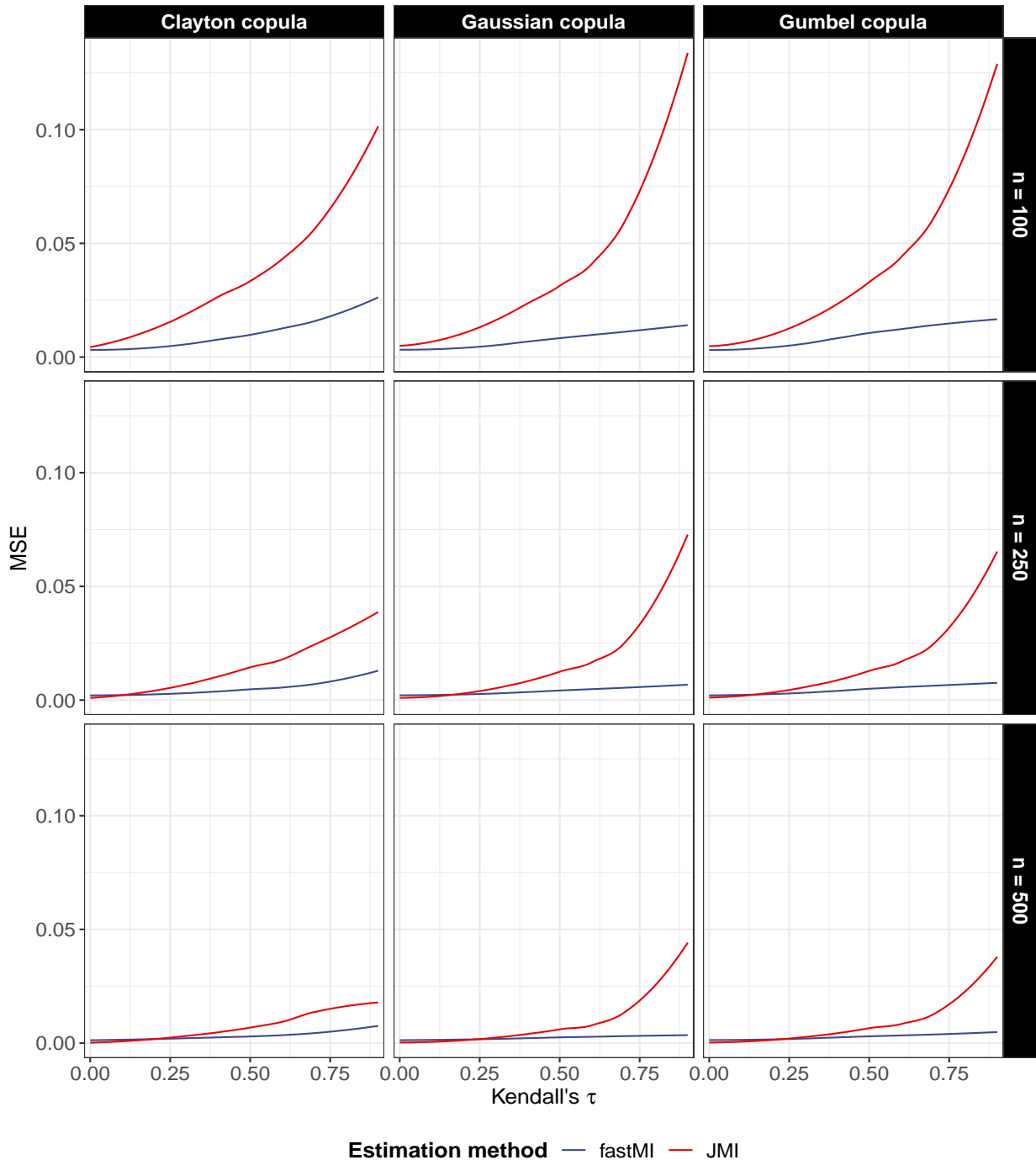


Fig. 1: In each panel, the lines represent mean squared errors (MSE) (y-axis) of different estimation methods based on $r = 1000$ replications for various levels of association controlled by Kendall's τ (x-axis). Correspondence between colors and the methods are as follows: **JMI in red** and **fastMI in blue**.

Comparison of empirical power of competing mutual information (MI) estimation methods for various association patterns.

The estimation methods compared here are Fast Fourier Transform–based MI (fastMI), the jackknifed MI (JMI) and the maximal information coefficient (MIC).

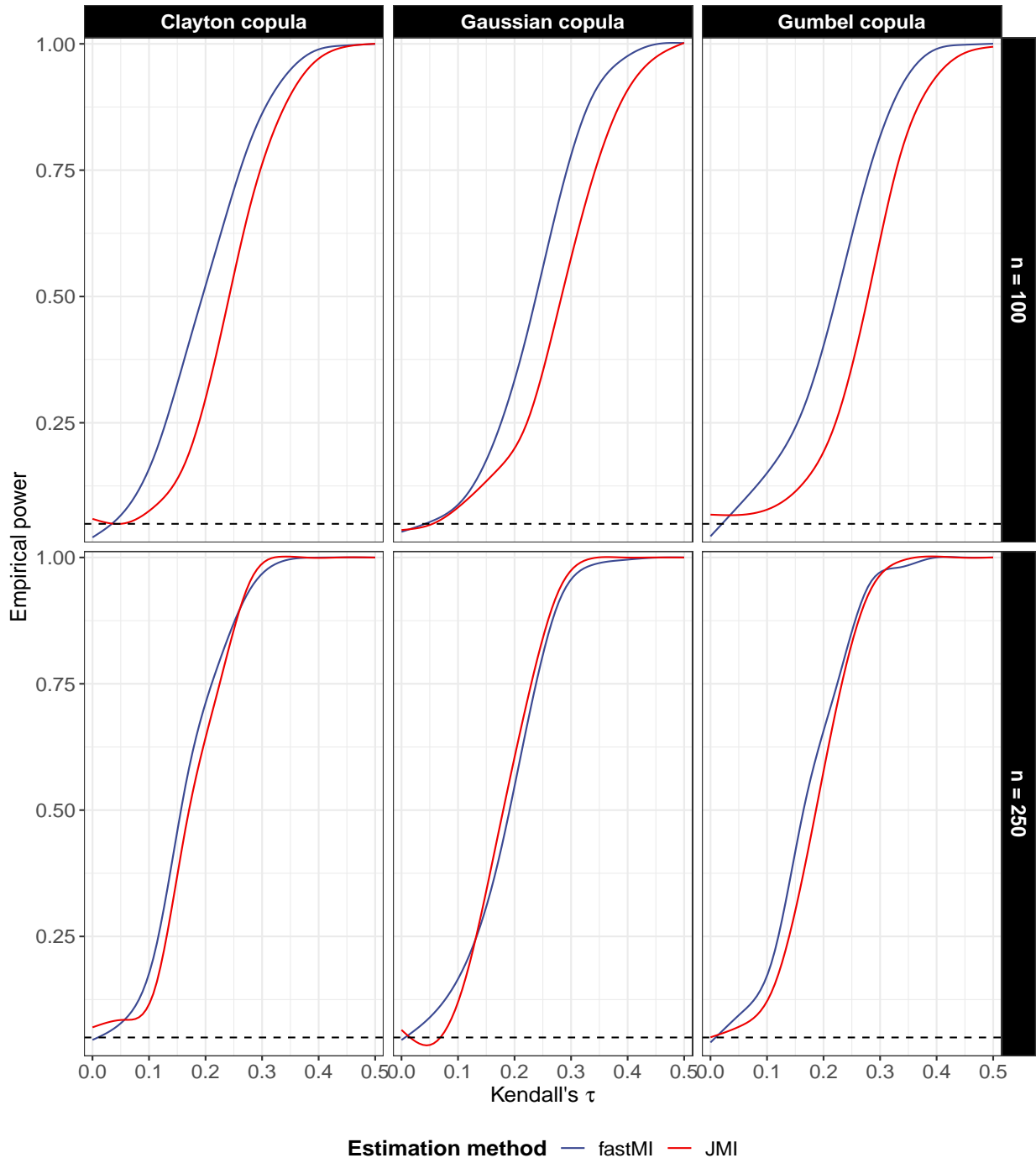


Fig. 2: In each panel, the lines represent the empirical power of tests at significance level $\alpha = 0.05$ for various levels of association controlled by Kendall's τ (x-axis). Dotted line parallel to x-axis denotes $\alpha = 0.05$. Correspondence between colors and the methods are as follows: JMI in red and fastMI in blue.

Transcript levels of the 35 genes that were detected by fastMI but not by JMI.

The methods compared here are Fast Fourier Transform–based MI (fastMI) and jackknifed MI (JMI).

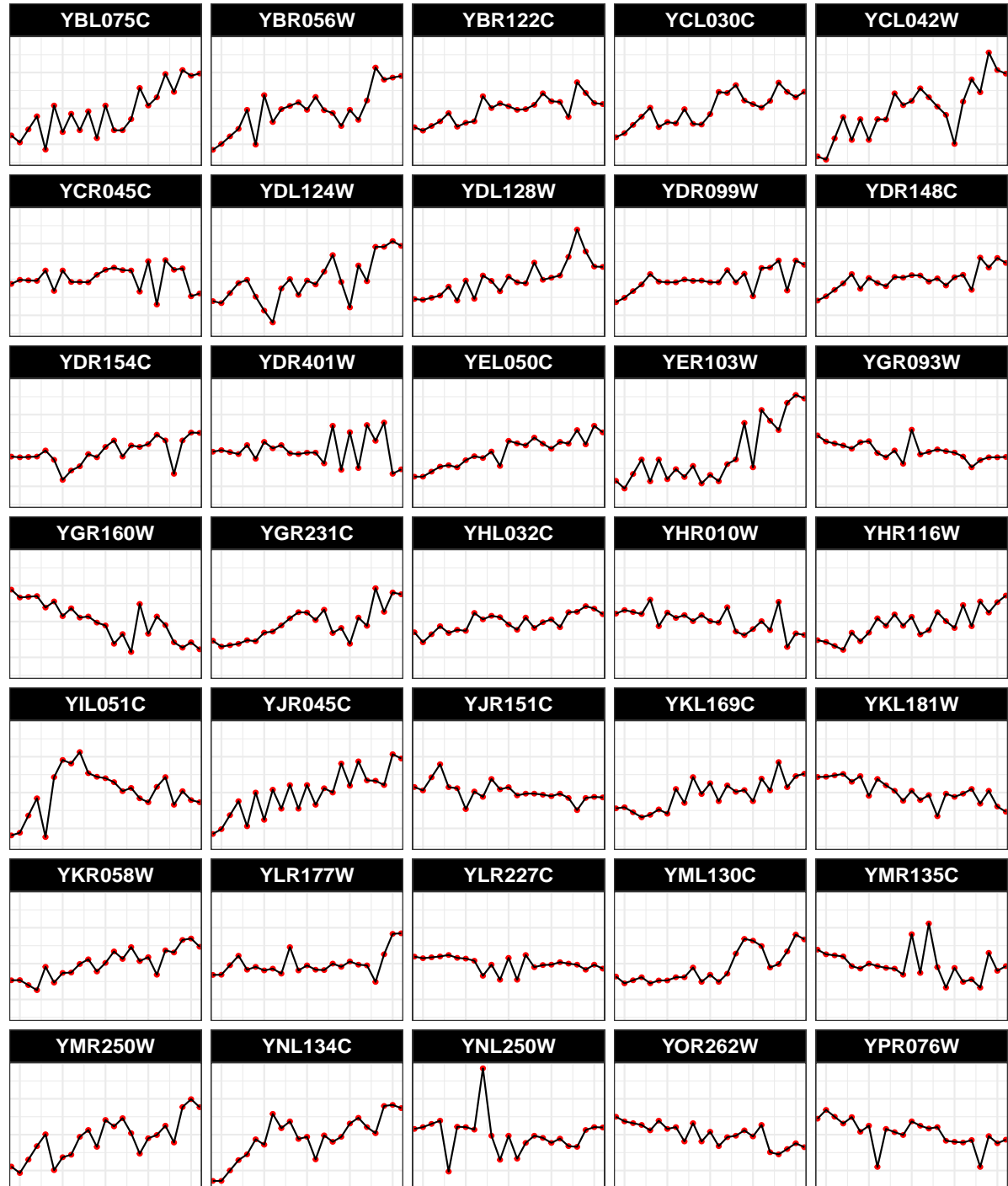


Fig. 3: In each panel, the lines depict oscillatory pattern of transcript levels (y-axis) of the 35 genes over time (x-axis) that were selected by fastMI but not JMI. The name of the gene is displayed on top of each panel.